

# Decreasing Ferroresonance Oscillation in Potential Transformers Including Nonlinear Core Losses by Connecting Metal Oxide Surge Arrester in Parallel to the Transformer

Hamid Radmanesh<sup>1</sup>, Mehrdad Rostami<sup>2</sup>

<sup>1</sup>Electrical Engineering Department, Aeronautical University of Science & Technology, Shahid Shamschiri Street, Karaj Old Road, Tehran, IRAN  
Tel: (+98-21)64032128, Fax: (+98-21)33311672

<sup>2</sup>Electrical Engineering Department, Shahed University, End of Khalij-e-Fars Highway, In front of Imam Khomeini holly shrine, Tehran-1417953836, IRAN  
Tel: (+98-21)51212020, Fax: (+98-21)51212021

<sup>1</sup>[Hamid.nsa@gmail.com](mailto:Hamid.nsa@gmail.com)

<sup>2</sup>[Rostami@shahed.ac.ir](mailto:Rostami@shahed.ac.ir)

---

**Abstract** – This paper studies the effect of MOV surge arrester on chaotic ferroresonance over voltages in potential transformer (PT) including nonlinear core losses effect. It is expected that MOV generally can cause ferroresonance 'dropout'. Time-domain study has been carried out to study this effect. Simulation has been done on a potential transformer rated 100VA, 275 kV. The magnetization characteristic of the transformer is modeled by a single-value two-term polynomial with order seven. The core loss is modeled by nonlinear resistance. Simulation results reveal that connecting the MOV in parallel with the potential transformer, exhibits a great controlling effect on ferroresonance over voltages. Phase plane, voltage waveforms, along with bifurcation diagrams are also derived. Significant effect on the onset of chaos, the range of parameter values that may lead to chaos along with ferroresonance over voltages has been obtained and presented. **Copyright © 2009 Praise worthy Prize S.r.l. - All rights reserved.**

**Keywords:** ferroresonance oscillation, stabilizing, chaos control, potential transformer, nonlinear core losses, MOV surge arrester

---

## I. Introduction

Ferroresonance occurs when a nonlinear inductor, usually a transformer with a saturable magnetic core, is excited through a linear capacitor from a sinusoidal source, particularly in the presence of long lines or capacitive power cables. It is usually initiated by a system disturbance of some form, for example, the disconnection of transformer feeder lines or the opening of a circuit breaker in series with a potential transformer. Also it can produce unpredictable over voltages and abnormal currents. The prerequisite for ferroresonance is a circuit containing nonlinear iron core inductance and some existed capacitance. The abrupt transition or jump from one state to another is triggered by a disturbance, switching action or a gradual change in values of a parameter. The first analytical work was done by Rudenberg in the 1940's [1]. More exacting and detailed work was done later by Hayashi in the 1950's [2]. Subsequent research has been divided into two main

areas: improving the transformer models and studying ferroresonance at the system level. Typical cases of ferroresonance are reported in [3]. One of the most possible cases which may happen is nonlinear iron core inductor that is fed by a series capacitor. These capacitances can be originated from several things, such as line-to-line capacitance, parallel lines, conductor to earth capacitance and circuit breaker grading capacitance [4]. Failure of electromagnetic potential transformer due to sustained overvoltage on switching\*/an in-depth field investigation and analytical study has been given in [5]. Fundamental theory of nonlinear dynamics and chaos can be found in [6], [7]. Controlling ferroresonance in voltage transformer by considering circuit breaker shunt resistance including transformer nonlinear core losses effect has been studied in [8]; this paper studies the effect of circuit breaker shunt resistance on the controlling chaotic ferroresonance in a voltage transformer while the core

losses of the voltage transformer core are highly nonlinear. It is expected that this resistance generally can cause ferroresonance 'dropout'. It has also been shown that chaotic ferroresonance states are not likely to occur under practical site conditions. C.B shunt resistance successfully can cause ferroresonance drop out and can control it, in the case of applying C.B shunt resistance system shows less sensitivity to initial condition and variation in system parameters. Tutorial Course on Digital Simulation of Transients in Power Systems has been given in [9]. The susceptibility of a ferroresonance circuit to a quasiperiodic and frequency locked oscillations are presented in [10], the effect of initial conditions is investigated in [11] in this reference, the solution of the nonlinear equation for a typical ferroresonant circuit containing a power transformer is shown to be dependent on the value of its initial conditions. It is also shown that a small change in initial conditions leads to a large difference in long-term behavior of the system, and this makes the future of the system unpredictable. Using a linear model, [12] has brought the Modeling and analysis guidelines for slow transients. Effect of circuit breaker grading capacitance on ferroresonance in PT is investigated in [13]. There are a number of documented cases of ferroresonance and a typical case is described in the references, for example in [14] Hopkinson performed system tests and simulations on the effect of different switching strategies on the initiation of ferroresonance in three phase systems. Frame [15] and others have developed piecewise-linear methods of modeling the nonlinearities in saturable inductances. Smith [16] categorized the modes of ferroresonance in one type of three phase distribution transformer based on the magnitude and appearance of the voltage waveforms. Arturi [17] and Mork [18] have demonstrated the use of duality transformations to obtain transformer equivalent circuits. In [19], the chaotic behavior of the simple power system is investigated for a range of loading conditions through computer simulations. The analysis of the severe over voltages caused by neutral shift and ferroresonance due to the disconnection of one phase of an ungrounded ye-delta transformer bank from the source is presented in [20]. The implications of applying MOV arresters in the distribution environment are described in [21], [22]. Performances of metal oxide arresters exposed to ferroresonance conditions in pad mount transformers are analyzed in [23], it has been pointed out that the arresters have a mitigating effect on the chaotic ferroresonance. An improved algorithm for generating the bifurcation diagrams of steady-state solutions to analyses chaotic ferroresonance in the presence of multiple nonlinearities has been reported in [24] modeling iron core nonlinearities is given in [25]. Effect of a connected MOV arrester in parallel to the power transformer is illustrated in [26]. Evaluation of chaotic ferroresonance in power transformers including

nonlinear core losses is investigated in [27]. Analysis of ferroresonance phenomena in power transformers including neutral resistance effect is investigated in [28]. Analysis of chaotic ferroresonance in transmission systems in the same right-of-way' has been done in [29]. A new method for partial discharge localization using multi-conductor transmission line model in transformer winding was given in [30]. Studies to utilize calculated condition information and measurements for transformer condition assessment have been investigated in [31]. Thermal capacitance calculation of top-oil temperature for power transformers was given in [32]. Sympathetic inrush phenomenon on power transformers and fault identification using artificial neural network is in [33]. Finally, effect of circuit breaker shunt resistance on chaotic ferroresonance in voltage transformer has shown in [34], in this work ferroresonance has been controlled by considering C.B resistance effect, C.B shunt resistance successfully can cause ferroresonance drop out and can control it, in the case of applying C.B shunt resistance system shows less sensitivity to initial condition and variation in system parameters. In all previous studies, the effect of MOV surge arrester on ferroresonance phenomena in potential transformer has been neglected. Current paper studies the effect of MOV on the global behavior of a PT ferroresonance circuit in potential transformer while its core losses have a nonlinear behavior.

## II. System Modeling Without MOV

During Potential Transformer (PT) ferroresonance an oscillation occurs between the nonlinear iron core inductance of the PT and existing capacitances of network. In this case, energy is coupled to the nonlinear core of the potential transformer via the open circuit breaker grading capacitance or system capacitance to sustain the resonance. The result may be saturation in the PT core and very high voltage up to 4p.u can theoretically gained in worst case conditions. The magnetizing characteristic of a typical 100VA PTs can be presented by 7 order polynomial [34]. These PTs fed through circuit breaker grading capacitance, and studied using nonlinear dynamics analysis and packages such as Rung KUTTA FEHLBERG algorithm and MATLAB SIMULINK. Fig.1 shows the single line diagram of the most commonly encountered system arrangement that can give rise to PT ferroresonance [30]. Ferroresonance can occur upon opening of disconnector 3 with circuit breaker open and either disconnector 1 or 2 closed. Alternatively it can also occur upon closure of both disconnectors 1 or 2 with circuit breaker and disconnector 3 open [34].

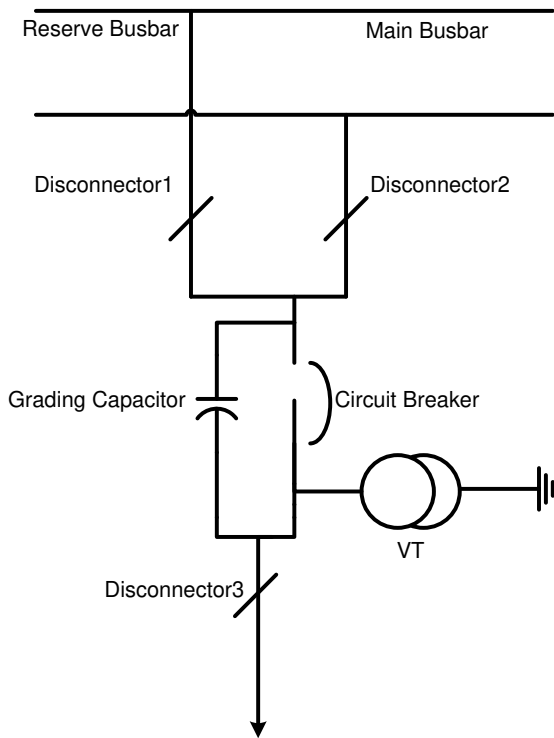


Fig.1. System one line diagram arrangement resulting to PT Ferroresonance

The system arrangement shown in Fig. 1 can effectively be reduced to an equivalent circuit as shown in Fig. 2.

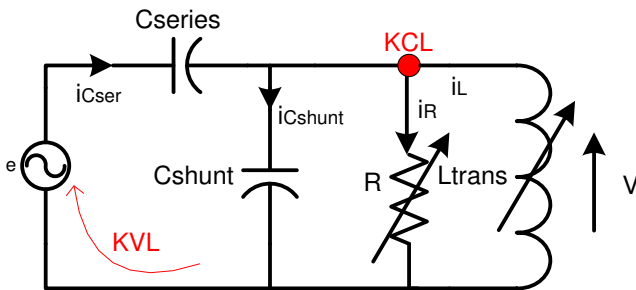


Fig.2. Basic reduced equivalent ferroresonance circuit [8]

In Fig. 2,  $E$  is the RMS supply phase voltage,  $C_{series}$  is the circuit breaker grading capacitance and  $C_{shunt}$  is the total phase-to-earth capacitance of the arrangement. The resistor  $R$  represents a potential transformer core loss that has been found to be an important factor in the initiation of ferroresonance and has been considered as a nonlinear resistance in this paper. In the peak current range for steady-state operation, the flux-current linkage can be approximated by a linear characteristic such as  $i_L = a\lambda$  where the coefficient of the linear term ( $a$ ) corresponds closely to the reciprocal of the inductance ( $a \cong 1/L$ ). However, for very high currents the iron core might be driven into saturation and the flux-current characteristic becomes highly nonlinear,

here the  $\lambda - i$  characteristic of the potential transformer is modeled as in [34] by the polynomial

$$i = a\lambda + b\lambda^7 \tag{1}$$

Where  $a = 3.14$ ,  $b = 0.41$

The polynomial of order seven and the coefficient  $b$  of equation (1) are chosen for the best fit of the saturation region. Fig (3) shows the comparison between different approximations of saturation region against the true magnetization characteristic that was obtained from field measurement by Dick and Watson [3], using a polynomial of order less than eleven to present the magnetization curve might be adequate for small capacity transformers such as potential transformer, but it does not sharply enough at the knee point to satisfy the magnetization characteristic of modern highly capacity transformers. In [8], the effect of changing the exponent of the nonlinear term on the modes of behavior of the ferroresonance circuit was investigated. It was found that for adequate representation of the saturation characteristics of a potential transformer core, the exponent  $q$  may acquire value 7 [8]. Fig (3) Shows these iron core characteristic for  $q=5, 7, 9$  and 11. The basic potential transformer ferroresonance circuit of Fig (2) can be presented by a differential equation. Because of the nonlinear nature of the transformer magnetizing characteristics, the behavior of the system is extremely sensitive to change in system parameter and initial conditions. A small change in the value of system voltage, capacitance or losses may lead to dramatic change in the behavior of it. A more suitable mathematical language for studying ferroresonance and other nonlinear systems is provided by nonlinear dynamic methods. Mathematical tools that are used in this analysis are phase plan diagram, time domain simulation and bifurcation diagram.

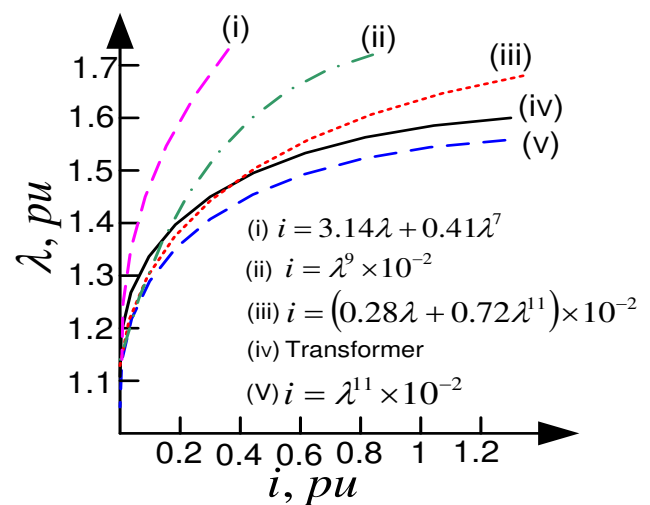


Fig.3. Nonlinear characteristics of transformer core with different values of  $q$  [8]

### III. System Dynamic and Equation

In this paper, the core loss model adopted is described by a third order power series which coefficients are fitted to match the hysteresis and eddy current nonlinear characteristics given in [9]:

$$i_{Rm} = h_0 + h_1 V_m + h_2 V_m^2 + h_3 V_m^3 \quad (2)$$

Per unit value of ( $i_{Rm}$ ) is given in table (1)

Table (1): parameters value of nonlinear core model [9]

core losses' Parameters	$h_0$	$h_1$	$h_2$	$h_3$
Per unit values	-0.000001	0.0047	-0.0073	0.0039

Mathematical analysis of equivalent circuit by applying KVL and KCL laws has been done and Equations of system can be presented as below:

$$\lambda_{peak} = \sqrt{2} \frac{v_{RMS}}{\omega} \quad (3)$$

$$v_L = \frac{d\lambda}{dt} \quad (4)$$

$$v_{C_{ser}} = e - v_L \quad (5)$$

$$e = \sqrt{2} E \sin \omega t \quad (6)$$

$$i = C_{ser} \frac{d(e - v_L)}{dt} = C_{ser} \left( \dot{e} - \frac{d^2 \lambda}{dt^2} \right) \quad (7)$$

$$i_1 = C_{sh} \frac{dv_L}{dt} = C_{sh} \frac{d^2 \lambda}{dt^2} \quad (8)$$

$$i_2 = h_0 + h_1 V_L + h_2 V_L^2 + h_3 V_L^3 \quad (9)$$

$$i_3 = a\lambda + b\lambda^7 \quad (10)$$

$$i = i_1 + i_2 + i_3 \Rightarrow C_{ser} \left( \sqrt{2} E \omega \cos \omega t - \frac{d^2 \lambda}{dt^2} \right) = C_{sh} \frac{d^2 \lambda}{dt^2} + (h_0 + h_1 v_L + h_2 v_L^2 + h_3 v_L^3) + (a\lambda + b\lambda^7) \sqrt{2} C_{ser} E \omega \cos \omega t \quad (11)$$

$$\frac{C_{sh}}{(C_{ser} + C_{sh})} (\sqrt{2} E \cos \omega t) = \frac{1}{\omega} \frac{d^2 \lambda}{dt^2} + \frac{1}{\omega(C_{ser} + C_{sh})} (h_0 + h_1 v_L + h_2 v_L^2 + h_3 v_L^3 a\lambda + b\lambda^7) \quad (12)$$

Where  $\omega$  is supply frequency, and E is the RMS supply phase voltage,  $C_{series}$  is the circuit breaker grading capacitance and  $C_{shunt}$  is the total phase-to-earth

capacitance of the arrangement and in (1)  $a=3.4$  and  $b=0.41$  are the seven order polynomial sufficient[34]. The state-space formulation  $\lambda$  and  $v$  as state variables is as

$$\begin{cases} x_1(t) = \lambda \\ x_2(t) = \dot{x}_1(t) \\ v = d\lambda / dt \\ x_2(t) = v \end{cases} \quad (13)$$

$$\dot{x}_2(t) = -\frac{1}{(c_{series} + c_{shunt})} (h_0 + h_1 x_2(t) + h_2 x_2(t)^2 + h_3 x_2(t)^3) - \frac{1}{c_{series} + c_{shunt}} (a x_1(t) + b x_1(t)^7) + \left( \frac{c_{series}}{c_{shunt} + c_{series}} \right) \omega E \sqrt{2} \cos \omega t \quad (14)$$

$$\begin{bmatrix} \dot{x}_1(t) \\ \dot{x}_2(t) \end{bmatrix} = \begin{bmatrix} 0 & 1 \\ -\frac{a - b x_1(t)^6}{c_{series} + c_{shunt}} & -\frac{(h_1 + h_2 x_2(t) + h_3 x_2(t)^2)}{(c_{series} + c_{shunt})} \end{bmatrix}$$

$$\begin{bmatrix} x_1(t) \\ x_2(t) \end{bmatrix} + \begin{bmatrix} 1 \\ 1 \end{bmatrix} u \quad (15)$$

$$\begin{bmatrix} u_1 \\ u_2 \end{bmatrix} = \begin{bmatrix} -\frac{h_0}{c_{series} + c_{shunt}} \\ \left( \frac{c_{series}}{c_{series} + c_{shunt}} \right) \omega E \sqrt{2} \cos(\omega t) \end{bmatrix} \quad (16)$$

$$y(t) = CX(t) \quad (17)$$

$$y(t) = v(t) = \begin{bmatrix} 0 & 1 \end{bmatrix} \begin{bmatrix} x_1(t) \\ x_2(t) \end{bmatrix} \quad (18)$$

$$\det \begin{bmatrix} \lambda & -1 \\ \frac{a + b(x_1(t))^6}{c_{series} + c_{shunt}} \lambda + \frac{(h_1 + h_2 x_2(t) + h_3 x_2(t)^2)}{(c_{series} + c_{shunt})} & \lambda \end{bmatrix} = 0 \quad (19)$$

$$\det[\lambda I - A] = 0 \quad (20)$$

$$\lambda^2 + p\lambda + q = 0 \quad \lambda_{1,2} = \frac{-p \pm \sqrt{p^2 - 4q}}{2} \quad (21)$$

Parameters value that was considered for simulation of state space was given in table (2).

Table (2): parameters value of the system elements

Parameter	Actual value	Per unit value
E	275kv	1 p.u
w	377 rad/sec	1 p.u
C <sub>series</sub>	0.5 nf	39.959 p.u
C <sub>shunt</sub>	0.1nf	7.92 p.u
α	-	25
k	-	2.5101

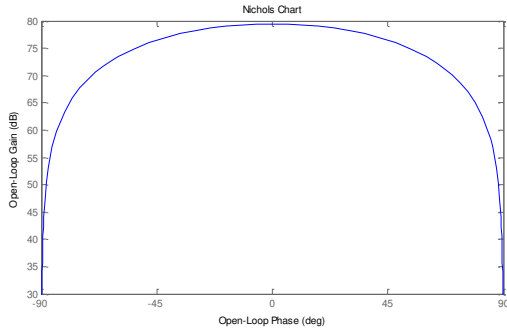


Fig.4. Nichols chart of the given parameters

### IV. Metal Oxide Surge Arrester Model

Surge Arrester is highly nonlinear resistor used to protect power equipment against over voltages. MOV can be arranged by cascading several metal oxide discs inside the same porcelain housing due to required protecting voltage. Size of each disc is related to its power dissipation capacity. The nonlinear V-I characteristic of each column of the surge arrester is modeled by combination of the exponential functions of the form

$$\frac{V}{V_{ref}} = K_i \left( \frac{I}{I_{ref}} \right)^{1/\alpha_i} \quad (22)$$

Where: V represents resistive voltage drop, I represents arrester current and K is constant and α is nonlinearity constant. This V-I characteristic is represented as follows:

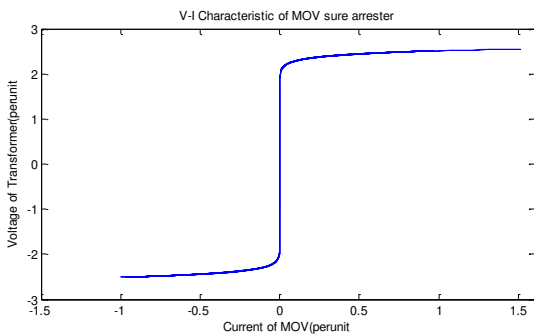


Fig 5. V-I characteristic of MOV surge arrester

The Surge Arrester block is modeled as a current source driven by the voltage appearing across its

terminals. Therefore, it cannot be connected in series with an inductor or another current source. As the Surge Arrester block is highly nonlinear, a robust integrator algorithm must be used to simulate the circuit. MATLAB ode23t with default parameters usually gives the best simulation speed. For continuous simulation, in order to avoid an algebraic loop, the voltage applied to the nonlinear resistance is filtered by a first-order filter with a time constant of 0.01 microseconds. This fast time constant does not significantly affect the result accuracy.

### V. System Modeling With MOV

Connecting MOV to the system in Fig.2, circuit can be driven in Fig 6.

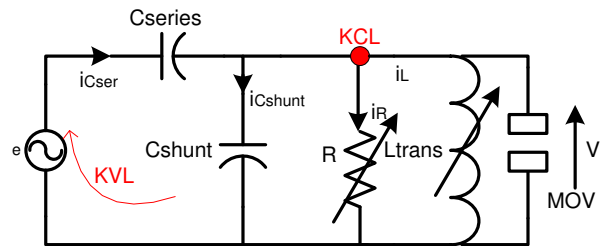


Fig.6. Basic reduced equivalent ferroresonance circuit with MOV

Linear approximation of the peak current of the magnetization reactance can be presented by equation (22):

$$i_L = a\phi \quad (23)$$

However, for very high currents, the iron core might be saturated where the flux-current characteristic becomes highly nonlinear.

Arrester can be expressed by the so-called "alpha" equation:

$$V = KI^{1/\alpha} \quad (24)$$

The differential equation for the circuit in fig (6) can be modified as follows:

$$\begin{aligned} \frac{C_{sh}}{(C_{ser} + C_{sh})} (\sqrt{2}E \cos \omega t) &= \frac{1}{\omega} \frac{d^2 \lambda}{dt^2} + \\ \frac{1}{\omega(C_{ser} + C_{sh})} (h_0 + h_1 v_L + h_2 v_L^2 + h_3 v_L^3 + a\lambda + b\lambda^7) &+ \\ + \frac{1}{C_{series}} \left( \frac{d\lambda}{kdt} \right)^\alpha & \end{aligned} \quad (25)$$

Where ω represents the power frequency and E is the peak value of the voltage source, shown in fig (2). The state-space formulation λ and v as state variables is as

$$\begin{cases} x_1(t) = \lambda \\ x_2(t) = \dot{x}_1(t) \\ v = d\lambda / dt \\ x_2(t) = v \end{cases} \quad (26)$$

$$\begin{aligned} \dot{x}_2(t) = & -\frac{1}{(c_{series} + c_{shunt})} (h_0 + h_1x_2(t) + h_2x_2(t)^2 + h_3x_2(t)^3) \\ & - \frac{1}{c_{series} + c_{shunt}} (ax_1(t) + bx_1(t)^7) - \frac{1}{c_{series}} \left(\frac{1}{k}\right)^\alpha x_2(t)^\alpha + \\ & \left(\frac{c_{series}}{c_{shunt} + c_{series}}\right) \omega E \sqrt{2} \cos \omega t \end{aligned} \quad (27)$$

$$\begin{aligned} \begin{bmatrix} \dot{x}_1(t) \\ \dot{x}_2(t) \end{bmatrix} = & \begin{bmatrix} 0 & 1 \\ -\frac{a-bx_1(t)^6}{c_{series} + c_{shunt}} & -\frac{(h_1 + h_2x_2(t) + h_3x_2(t)^2)}{(c_{series} + c_{shunt})} - \frac{1}{c_{series}} \left(\frac{1}{k}\right)^\alpha x_2(t)^{\alpha-1} \end{bmatrix} \\ \begin{bmatrix} x_1(t) \\ x_2(t) \end{bmatrix} + & \begin{bmatrix} 1 \\ 1 \end{bmatrix} u \end{aligned} \quad (28)$$

$$\begin{bmatrix} u_1 \\ u_2 \end{bmatrix} = \begin{bmatrix} -\frac{h_0}{c_{series} + c_{shunt}} \\ \left(\frac{c_{series}}{c_{series} + c_{shunt}}\right) \omega E \sqrt{2} \cos(\omega t) \end{bmatrix} \quad (29)$$

$$y(t) = CX(t) \quad (30)$$

$$y(t) = v(t) = \begin{bmatrix} 0 & 1 \end{bmatrix} \begin{bmatrix} x_1(t) \\ x_2(t) \end{bmatrix} \quad (31)$$

$$\det[\lambda I - A] = 0 \quad (32)$$

$$\lambda^2 + p\lambda + q = 0 \quad \lambda_{1,2} = \frac{-p \pm \sqrt{p^2 - 4q}}{2} \quad (33)$$

For parameters value of table (2) plus MOV parameters, bode diagram has been simulated and has been shown in fig (7).

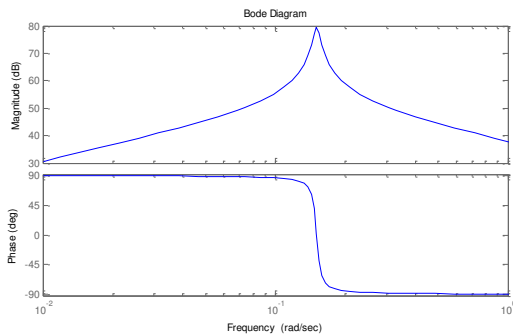


Fig.7. Bode diagram of the given parameters of table (2)

## VI. Simulation Results

Equations (12) and (25) contain a nonlinear term and do not have simple analytical solution. So the equations were solved numerically using an embedded RUNGE-KUTTA FEHLBERG algorithm with adaptive step size control. Values of E and  $\omega$  were fixed by 1 p.u., corresponding to AC supply voltage and frequency.  $C_{series}$  is the CB grading capacitance and its value obviously depends on the type of circuit breaker which is used. In this analysis  $C_{series}$  is assumed 0.5nF and  $C_{shunt}$  vary between 0.1nF to 3nF. Initial condition are  $V(t) = \sqrt{2}$ ,  $\lambda(t) = 0$  at  $t=0$ , representing circuit breaker operation at maximum voltage. In this state, system for both cases, with and without MOV has been simulated for  $E=1, 4$  p.u. The studied system has a periodic behavior for  $E=1$  p.u and chaotic behavior for  $E=4$  p.u while by applying MOV, system behavior remains periodic for  $E=1$  p.u and  $E=4$  p.u.

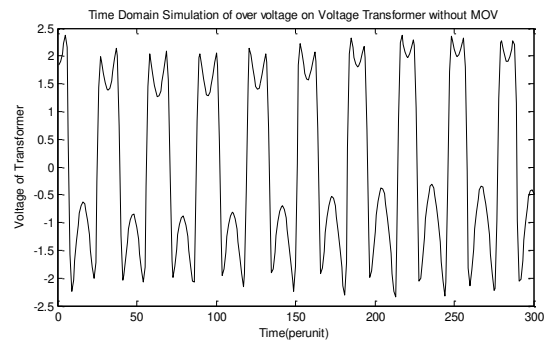


Fig.8. Time domain simulation for fundamental resonance motion without MOV surge arrester

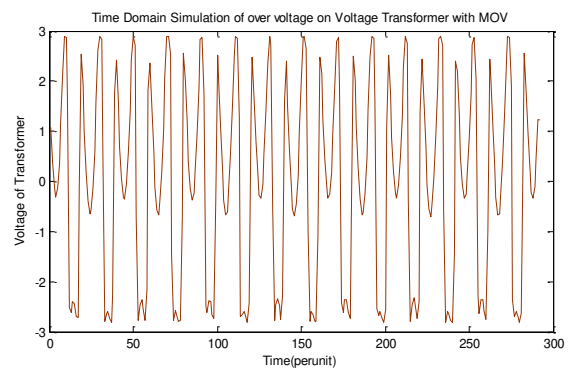


Fig.9. Time domain simulation for period2 motion with MOV surge arrester

Figs.8 and 9 show time domain simulation for these two cases that represented the fundamental resonance and sinusoidal voltage wave form with a frequency equal to the power system frequency, Figs.10 and 11 show the simulation result for  $E=4$  p.u including MOV and without considering MOV surge arrester. By referring to

fig.11 and comparing with fig.10, it is shown the MOV surge arrester clamp the over voltages from 6p.u to 3p.u and after transient signal, its behavior reaches to the normal condition.

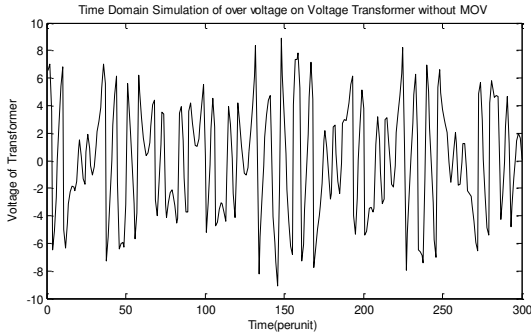


Fig.10. Time domain simulation for chaotic motion without MOV

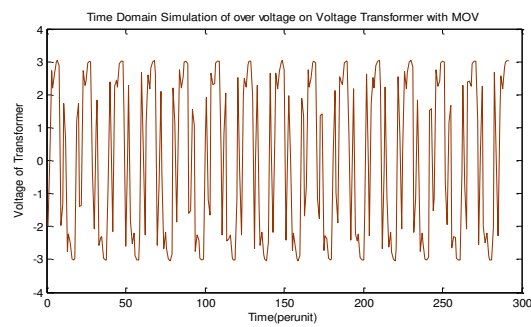


Fig.11. Time domain simulation for subharmonic resonance motion with MOV surge arrester

Corresponding phase plan diagrams has been shown the effect of the MOV to damp the over voltages and it is shown in figs.12, 13 for  $E=1$  p.u and figs.14 and 15 for  $E=4$  p.u. it obviously shows that MOV clamp the ferroresonance overvoltage and keep it in  $E=2.5$  p.u.

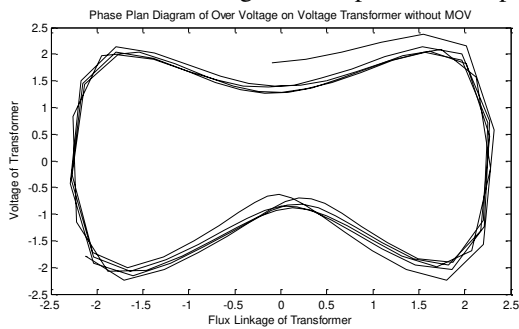


Fig.(12.a). Phase plan diagram for fundamental resonance motion without MOV surge arrester

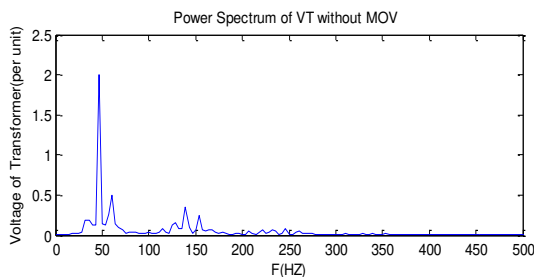


Fig.(12.b).power spectrum of PT without MOV for fundamental resonance

Corresponding phase plan diagrams has been shown apparent the MOV effect which is shown in figs. (13.a) and (13.b) for  $E=1$ p.u, and phase plan that has been shown in fig.14, when the overvoltage's reaches up to 6 p.u by applying MOV in parallel, overvoltage's reaches to the 2.5 p.u according to the fig.15, also power spectrum of the corresponding phase plan diagrams clearly show magnitude of the existing resonance in the system.

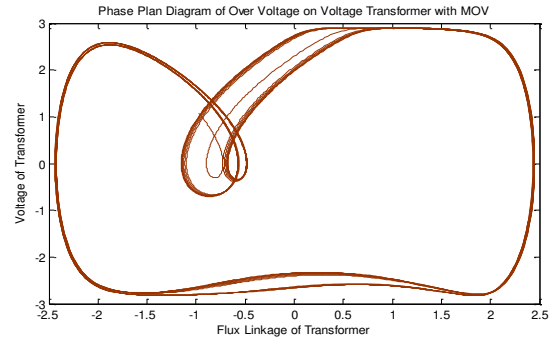


Fig.(13.a). Phase plan diagram for period2 motion with MOV surge arrester

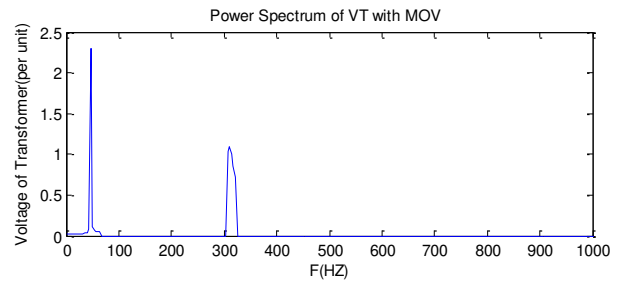


Fig.(13.b). Power spectrum of PT including MOV for period2 oscillation

It is obviously shows that MOV clamp the ferroresonance overvoltage and keep it in  $E=2.5$  p.u. System parameters are as below:

Table (2). Parameters value that has been considered for simulation

Parameter	Actual value	Per unit value
E	275kv	1 p.u
w	377 rad/sec	1 p.u
C <sub>series</sub>	0.5 nf	39.959 p.u
C <sub>shunt</sub>	1.25nf	98p.u

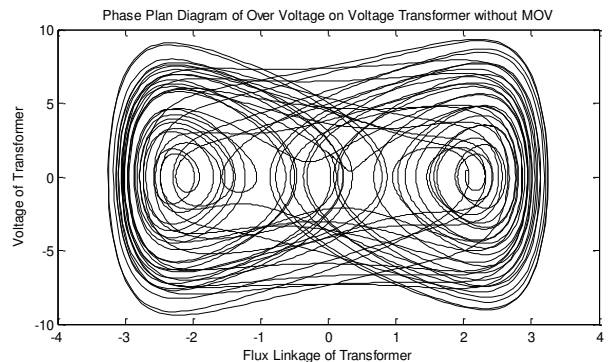


Fig.(14.a). Phase plan diagram for chaotic motion without considering MOV surge arrester

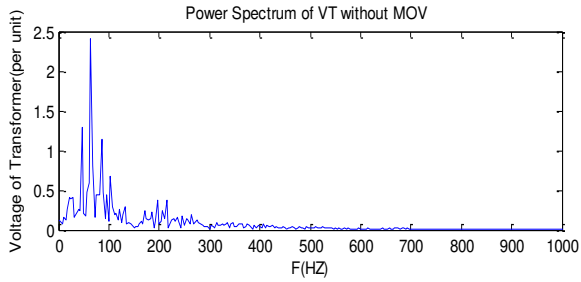


Fig.(14.a). Power spectrum of PT without MOV for chaotic oscillation

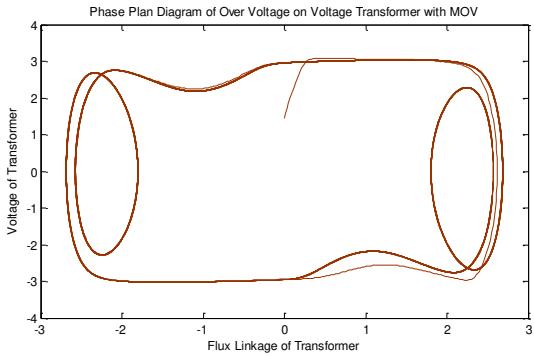


Fig.(15.a). Corresponding phase plan diagram for period2 motion with applying MOV corresponding by fig.(14.a)

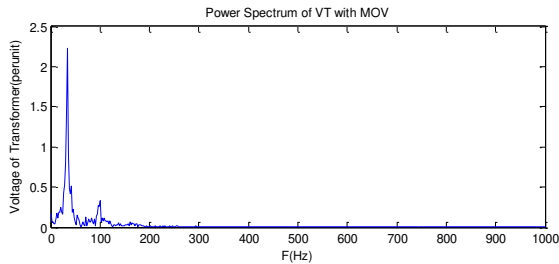


Fig.(15.a). Power spectrum of PT without considering MOV surge arrester

Another tool that was used for solving the nonlinear equation of studied system is bifurcation diagram. In this paper, it is shown the effect of variation in the voltage of the system on the ferroresonance overvoltage in the PT, and finally the effect of applying MOV on this overvoltage by the bifurcation diagrams. By using the bifurcation diagrams, fig (16) clearly shows the ferroresonance overvoltage in PT when voltage of system increase up to 4p.u.

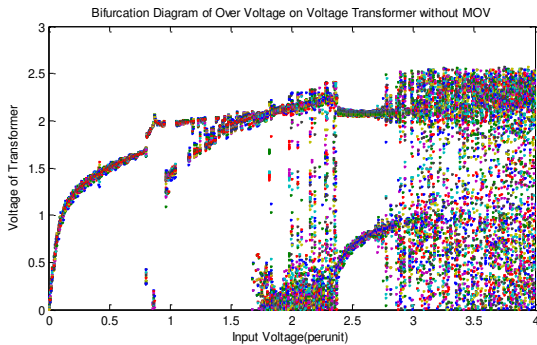


Fig.16. Bifurcation diagram for voltage of transformer versus voltage of system, without considering MOV surge arrester

System parameters are as follows:

Table (4): Parameter value that has been considered for simulation

Parameter	Actual value	Per unit value
E	275kv	1 p.u
$\omega$	377 rad/sec	1 p.u
C <sub>series</sub>	0.5 nf	39.959 p.u
C <sub>shunt</sub>	0.1nf	7.92 p.u
R <sub>core</sub>	Nonlinear model	Nonlinear model

In fig.17 when E=0.25 p.u, voltage of PT has a chaotic behavior, in E=2.2p.u, period1 appears and in E=3p.u period3 has been begun, after that remains in the linear manner. Corresponding bifurcation diagram by fig.16 with the same parameter while MOV parameters have been added to the simulation has been shown in this figure.17.

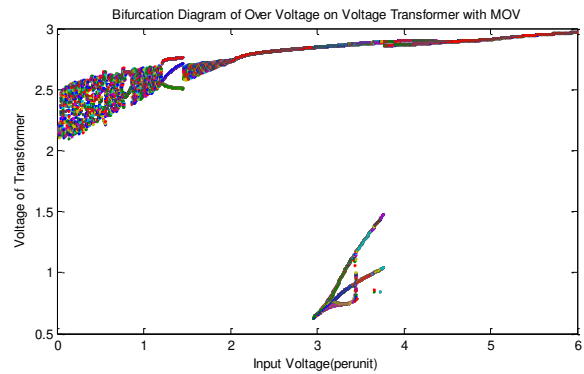


Fig.17. Bifurcation diagram for voltage of transformer versus voltage of system with applying MOV

It is shown that by applying MOV, system behaviors coming out from chaotic region and MOV clamp the overvoltage from 8 p.u to 2.2 p.u.

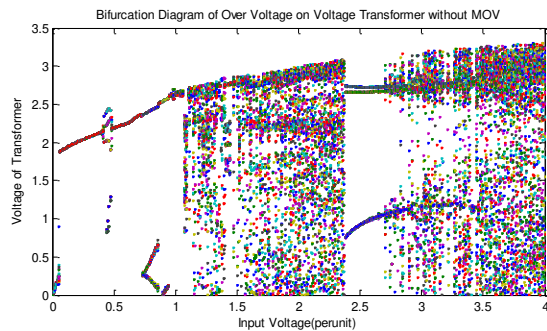


Fig.18. Bifurcation diagram for voltage of transformer versus voltage of system, without considering MOV surge arrester

It is shown that system behavior has period doubling bifurcation logic and there are many resonances in the system behavior. Bifurcation diagram with the same parameter in the case of MOV to the PT is shown in fig.19



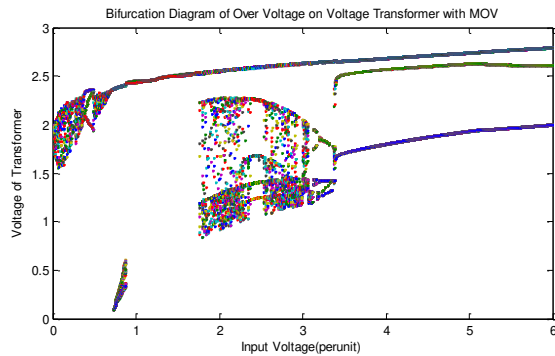


Fig.19. Bifurcation diagram for voltage of transformer versus voltage of system, corresponded by fig.15 with applying MOV

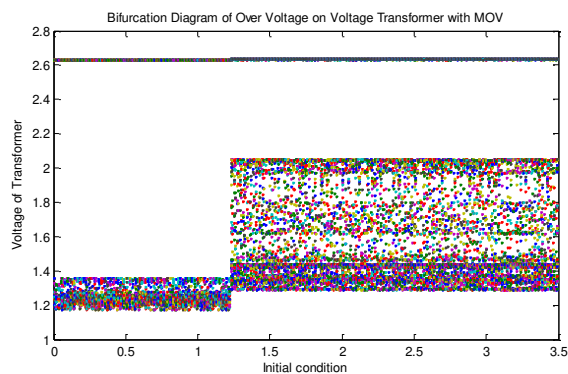


Fig.20. Bifurcation diagram for initial condition, with applying MOV

Bifurcation diagram of fig.(20) clearly shows effect of changing initial condition on the global behavior of the potential transformer ferroresonance by increasing initial condition value from 0 to 3.5p.u, ferroresonance over voltages has been increased and one jump has been occurred in the trajectory of the system, suddenly value of over voltage jumps from 1.4p.u to 2.1p.u, this changing in the value of over voltages have been increased if MOV surge arrester has not been considered in parallel with potential transformer.

Table (5): Parameter value for simulation of figs. 18, 19

Parameter	Actual value	Per unit value
E	275kv	1 p.u
w	377 rad/sec	1 p.u
C <sub>series</sub>	0.5 nf	39.959 p.u
C <sub>shunt</sub>	0.19nf	15.042 p.u
$\alpha$	-	25
k	-	2.5101

According to the parameters, it is shown that by changing the C<sub>series</sub> from 0.1nf to 0.19nf, ferroresonance overvoltage greatly changes and plot of fig.18 is completely different by fig.16. In this figure when trajectory of system is in E=1 p.u, its behavior begin the period1, in E=1.8 p.u, suddenly resonance take place and system goes to chaotic region and when input voltage reached to 3.5 p.u, the system behavior coming out from chaos. By applying MOV in this case, it is

shown that MOV has great effect on this overvoltage and successfully cause ferroresonance drop out. In the real systems, maximum overvoltage that PT can withstand is 4p.u, and if over voltages cross it, PT failure follows.

## VII. Conclusions

Chaotic ferroresonance cannot be ruled out in a de energized line in the same right-of-way as a parallel energized line for normal distances and operating procedures. Transformer -core saturation plays a decisive role in determining the type of ferroresonance oscillation. Potential Transformers fed through circuit breaker grading capacitance have been shown exhibiting fundamental frequency and chaotic ferroresonance conditions similar to high capacity power transformers fed via capacitive coupling from nearby sources like parallel transmission lines. Simulations have shown that a change in the value of the equivalent line to ground capacitance, may originate different types of ferroresonance over voltages. It has also been shown that chaotic ferroresonance are not likely to occur under practical conditions but if it occurs, MOV successfully can cause ferroresonance drop out. In the case of applying MOV, system shows less sensitivity to initial conditions and variation in system parameters. The presence of the arrester tends to clamp the ferroresonance. The system shows a greater tendency for chaos saturation characteristics with lower knee point, which corresponds to higher values of exponent q. the arrester successfully eliminates chaos for exponent q=7. Different system capacitances and resistances has been studied but not shown in this paper. Variation of the system capacitance reveals that quasiperiodic oscillations (route to chaos) occurred rather than period doubling bifurcation. To continue this study, one may include nonlinear core model and enhance extracted results.

## References

- [1] R. Rudenberg, *Transient Performance of Electric Power Systems*. New York, NY: McGraw-Hill Book Company, 1950, ch. 48.
- [2] C. Hayashi, *Nonlinear Oscillations in Physical Systems*. New York, NY: McGraw-Hill Book Company, 1964.
- [3] DICK, E.P., and WATSON, W.: 'Transformer models for transient studies based on field measurement', *IEEE Trans.*, 1981, PAS-100, pp. 409-417.
- [4] E.J. Dolan, D.A. Gillies, E.W. Kimbark, Ferroresonance in a transformer switched with an EVH line, *IEEE Transactions on Power Apparatus and Systems PAS-91* (1972) 1273\_/1280.
- [5] R.P. Aggarwal, M.S. Saxena, B.S. Sharma, S. Kumer, S. Krishan, Failure of electromagnetic voltage transformer due to sustained overvoltage on switching\*/an in-depth field investigation and analytical study, *IEEE Transactions on Power Apparatus and Systems PAS-100* (1981) 4448\_/4455.
- [6] C. Kiény, Application of the bifurcation theory in studying and understanding the global behavior of a ferroresonance electric power circuit, *IEEE Transactions on Power Delivery* 6 (1991)866\_/872.

- [7] A.E.Araujo, A.C. Soudack, J.R. Marti, Ferroresonance in power systems: chaotic behavior, IEE Proceedings-C 140 (1993) 237\_/240.
- [8] Radmanesh, Hamid, Controlling ferroresonance in voltage transformer by considering circuit breaker shunt resistance including transformer nonlinear core losses effect, *International Review on Modelling and Simulations (IREMOS) journal*, Vol. 3 N. 5, Part A, SEP-OCT 2010.
- [9] H.W. Dommel, A. Yan, R.J.O. De Marcano, A.B. Miliani, in:H.P. Khincha(Ed.), Tutorial Course on Digital Simulation of Transients in Power Systems (Chapter 14), IISc, Bangalore, 1983,pp. 17\_/38.
- [10]S.K.Chkravarthy, C.V.Nayar, 'Frequency-locked and quasi periodic (QP) oscillations in power systems', IEEE Transactions on Power Delivery 13 (1997) 560\_/569.
- [11] S.Mozaffari, M. Sameti, A.C. Soudack, Effect of initial conditions on chaotic ferroresonance in power transformers, IEE Proceedings\*/Generation, Transmission and Distribution 144(1997) 456\_/460.
- [12] IEEE Working Group on Modeling and Analysis of Systems Transients, M.R. Iravani, Chair, Modeling and analysis guidelines for slow transients\*/part III: the study of ferroresonance, IEEE Transactions on Power Delivery, 15 (2000) 255\_/265.
- [13] B.A.T. Al Zahawi, Z. Emin, Y.K. Tong, Chaos in ferroresonant wound voltage transformers: effect of core losses and universal circuit behavioral, IEE Proceedings\*/Sci. Meas.Technol. 145(1998) 39\_/43.
- [14] R. H. Hopkinson, "Ferroresonance during single-phase switching of 3-phase distribution transformer banks," *IEEE Trans. PAS*, vol. PAS-84, no. 4, pp. 289–293, Apr. 1965.
- [15] J. G. Frame, N. Mohan, and T. Liu, "Hysteresis modeling in an electromagnetic transients program," *IEEE Trans. PAS*, vol. PAS-101, no. 9, pp. 3403–3411, Sept. 1982.
- [16] D. R. Smith, S. R. Swanson, and J. D. Borst, "Over voltages with remotely-switched cable-fed grounded wye-wye transformers," *IEEE Trans. PAS*, vol. PAS-94, no. 5, pp. 1843–1853, Sept./Oct. 1975.
- [17] C.M.Arturi, 'Transient simulation and analysis of a five-limb generator step-up transformer following an out-of-phase synchronization', *IEEE Trans. Power Delivery*, vol. 6, no. 1, pp. 196–207, Jan. 1991.
- [18], "Ferroresonance and chaos—Observation and simulation of ferroresonance in a five-legged core distribution transformer," North Dakota State University, Ph.D. dissertation, Publication no. 9227588, UMI Publishing Services, Ann Arbor, MI 48106, (800) 521-0600, May 1992.
- [19] CHIANG, H.D., LIU, C.W., VARIYA, P.P, WU, F.F., and LAUBY, M.G.: 'Chaos in a simple power system', *IEEE Trans., Power Syst.*, 1993, 8, 940, pp. 1407-1417.
- [20] WALLING, R.A., HARTANAR, K., and ROS, W.J.: 'Self-generated over voltages due to open-phasing of ungrounded- wye delta transformer banks', *IEEE Trans. Power Deliv.*, 1995, 10, (1), pp. 526-531.
- [21] SHORT, T.A., BURKE, J.J., and MANCAO, R.T.: 'Application of MOVs in the distribution environment', *IEEE Trans. Power Deliv.*, 1994, 9, (1), pp. 293-305.
- [22] KERSHAW, S.S., GAIBROIS, K.B., and STUMP, K.B.: 'Applying metal-oxide surge arrester on distribution systems', *IEEE Trans. Power Deliv.*, 1989, 4, (1), pp. 301-307.
- [23] WALLING, R.A., HARTANA, R.K., RECKARD, R.M., SAMPART, M.P., and BALGLE, T.R.: 'Performance of metal oxide arresters exposed to ferroresonance pad mount transformer' *IEEE Trans. Power Deliv.*, 1994, 9, (2), pp.7888-795.
- [24] Al-Anbarri, K.: 'Some investigation into occurrence of chaotic ferroresonance in power system'. Ph.D. Thesis, Anna University,Dep. of Elec. & Electronic Eng., Chennai, India, March 2004.
- [25] W.L.A. Neves, H. Dommel, on modeling iron core nonlinearities, *IEEE Transactions on Power Systems* 8 (1993) 417\_/425.
- [26] K. Al-Anbarri, R. Ramanujam, T. Keerthiga, K. Kuppusamy, Analysis of nonlinear phenomena in MOV connected Transformers, *IEE Proceedings\*/Generation Transmission and Distribution*148 (2001) 562\_/566.
- [27] Abassi, A.; Rostami, M.; Radmanesh, H, Abbasi, H; "Evaluation of Chaotic Ferroresonance in power transformers including Nonlinear Core Losses," *IEEE International Conference on Environment and Electrical Engineering*, pages 220-224, Karpacz, May 10-13 2009. Available in [www.ICEE2011.com](http://www.ICEE2011.com)
- [28] Radmanesh, H.; Abassi, A.; Rostami, M.; , "Analysis of ferroresonance phenomena in power transformers including neutral resistance effect," *Southeastcon*, 2009. SOUTHEASTCON '09. IEEE , vol., no., pp.1-5, 5-8 March 2009doi:10.1109/SECON.2009.5233395 URL: <http://ieeexplore.ieee.org/stamp/stamp.jsp?tp=&arnumber=5233395&isnumber=5174034>
- [29]Lakshemi Naresh, S.: 'Analysis of chaotic ferroresonance in transmission systems in the same right-of-way'. ME Thesis, Anna University, Dep. of Elec. & Electronic Eng., Chennai, India, Dec 2002.
- [30] Shakeri, J.; Abbasi, A. H.; Shayegani, A. A.; Mohseni, H., A New Method for Partial Discharge Localization Using Multi-Conductor Transmission Line Model in Transformer Winding, *International Review of Electrical Engineering journal*, Vol. 4(Issue 3):470-476, MAY-JUN 2009.
- [31] Pylvanainen, Jouni; Nousiainen, Kirsi; Verho, Pekka, Studies to Utilize Calculated Condition Information and Measurements for Transformer Condition Assessment, *International Review of Electrical Engineering journal*, Vol. 4(Issue 4):684-689, JUL-AUG 2009.
- [32] Iskender, Ires; Mamizadeh, Ali, Thermal Capacitance Calculation of Top-Oil Temperature for Power Transformers, *International Review of Electrical Engineering journal*, Vol. 4(Issue 5):882-886, SEP-OCT 2009.
- [33] Sengul, M.; Ozturk, S.; Alboyaci, B., Sympathetic Inrush Phenomenon on Power Transformers and Fault Identification Using Artificial Neural Networks, *International Review of Electrical Engineering journal*, Vol. 4(Issue 5):1069-1075, SEP-OCT 2009.
- [34] H. Radmanesh, M. Rostami, "Effect of Circuit Breaker Shunt Resistance on Chaotic Ferroresonance in Voltage Transformer," *Advances in Electrical and Computer Engineering*, vol. 10, no. 3, pp. 71-77, 2010. [Online]. Available: <http://dx.doi.org/10.4316/AECE.2010.03012>.

## Authors' information



**Hamid Radmanesh** was born in 1981. He studied Telecommunication engineering at Malek e Ashtar industrial University Tehran, Iran, and received the BSC degree in 2006 also studied electrical engineering at Shahed University Tehran, Iran, and received the MSC degree in 2009. Currently, he is a lecturer of electrical engineering and teaches High Voltage Insulation Technology, Transient in Power System and Apparatus at Aeronautical University of Science& Technology. He is IEEE associate member. His research interests include Design and modeling of Power Electronic Converters, Drives, and Transient in power system, Chaos in power system apparatus.



**Mehrdad Rostami** was born in 1965, Tehran, IRAN. He received BSc, MSc and Ph.D in Electrical engineering from Tehran Polytechnic University (Amir Kabir), Tehran Iran in 1988, 1991 and 2003 respectively. He is currently working as an Assistant professor and vice chancellor in research and development of Shahed University Engineering Faculty, Tehran, IRAN.